

**N87 - 22709** :

**TRANSIENT RESPONSE FOR INTERACTION OF TWO DYNAMIC BODIES**

by

**A. Prabhakar & L.G. Palermo**

**Martin Marietta Michoud Aerospace, New Orleans, Louisiana**

**ABSTRACT**

During the launch sequence of any space vehicle complicated boundary interactions occur between the vehicle and the launch stand. At the start of the sequence large forces exist between the two; contact is then broken in a short but finite time which depends on the release mechanism. The resulting vehicle response produces loads which are very high and often form the design case. It is known that the treatment of the launch pad as a second dynamic body is significant for an accurate prediction of launch response.

A technique has been developed for obtaining loads generated by the launch transient with the effect of pad dynamics included. The method solves uncoupled vehicle and pad equations of motion. The use of uncoupled models allows the simulation of vehicle launch in a single computer run. There is no need for a second computer run to introduce compensating forces that are required to simulate detachment for coupled models. Modal formulation allows a closed-form solution to be written, eliminating any need for a numerical integration algorithm.

When the vehicle is on the pad the uncoupled pad and vehicle equations have to be modified to account for the constraints they impose on each other. This necessitates the use of an iterative procedure to converge to a solution, using Lagrange multipliers to apply the required constraints. As the vehicle lifts off the pad the coupling between the vehicle and the pad is eliminated point by point until the vehicle flies free.

Results obtained by this method have been shown to be in good agreement with observed loads and other analysis methods.

The resulting computer program is general, and has been used without modification to solve a variety of contact problems. The contact point description could be made more elaborate to include effects of friction, geometry, etc. By allowing the second body (it need not be a pad) to have rigid body free-free modes other problems, such as berthing/docking dynamics, could be tackled.

# TRANSIENT RESPONSE FOR INTERACTION OF TWO DYNAMIC BODIES

by

A. Prabhakar & L.G. Palermo

Martin Marietta Michoud Aerospace, New Orleans, Louisiana

## 1.0 INTRODUCTION

This paper describes a method of obtaining the transient response of two interacting dynamic bodies. The technique was developed originally to obtain the response during the launch sequence of the Space Shuttle Vehicle (SSV) from a dynamic launch pad. Because of the historical association with the SSV launch problem this paper presents the development from that particular viewpoint but it must be emphasised that the method is generally applicable, and the resulting computer code has been used in solving a variety of contact problems.

The launch event of any space vehicle causes complicated boundary interactions between the vehicle and the launch stand. At the start of the sequence large forces exist between the two; contact is then broken in a short but finite time which depends on the release mechanism. During this time the two may recontact as the loads are redistributed in the system. The vehicle response resulting from this non-linear transient phenomenon produces loads which often form the design case. It is known from experience that the use of a non-dynamic launch pad predicts loads that are too high. Therefore the treatment of the launch pad as a second dynamic body is significant for an accurate prediction of launch response.

A technique has been developed for obtaining loads generated by the launch transient with the effect of pad dynamics included (ref. 1). The method solves uncoupled vehicle and pad equations of motion. The use of uncoupled models allows the simulation of vehicle launch in a single computer run. There is no need for a second computer run to introduce compensating forces that are required to simulate detachment for coupled models. Modal formulation allows a closed-form solution to be written, eliminating any need for a numerical integration algorithm. However, an iterative procedure is required to solve the equations of motion when the two bodies are in contact.

Several other factors influence the response from the launch transient. A control system maintains a vertical vehicle attitude, zeroing out angular accelerations, by changing the direction of the thrust vector of the Solid Rocket Boosters (SRBs). Another source of large loads is from the constraints imposed on the cryogenic shrinkage of the External Tank (ET); these loads are relieved as the vehicle separates from the launch pad. Also important is a second order effect resulting from the offset centre of gravity of the vehicle. This offset c.g. would tend to induce greater structural deflection than can be obtained normally; we have termed this effect "gravity softening". Techniques for the proper simulation of these effects are discussed in the paper. An area for further development is to make the contact point description more elaborate to include the effects of friction, geometry, misalignment, etc.

Although in the development presented in this paper the pad is a grounded body, it could be made more general and have rigid body modes allowed. This would enable the technique to be used in calculating the berthing/docking dynamic response for the Space Station.

## NOMENCLATURE

$C_M$	Coupling mass term in Craig-Bampton formulation of analysis models.
$F$	Generalised force.
$F(t)$	Discrete time variant applied force.
$g$	Gravitational acceleration.
$h$	Integration interval.
$I$	Identity matrix
$K$	Stiffness matrix.
$M$	Mass matrix.
$M_B, K_B$	Boundary mass and stiffness terms in Craig-Bampton formulation.
$q$	Modal freedoms.
$RB$	Geometric rigid body modeshape.
$x$	Discrete freedoms.
$x_g$	Freedoms of the centre of gravity of the vehicle.
$\Phi$	Modeshapes matrix.
$\eta$	Error between successive iterations.
$\tau$	Time variation during an integration interval.
$\omega_n$	Natural frequency (radians/sec).
$\zeta$	Ratio of critical damping.

### Subscripts

$A$	Applied
$v$	Vehicle
$s$	Launch stand
$C$	Contact
$0$	Values at time zero (initial values)

### Superscripts

$T$	Transpose
$-1$	Inverse

## 2.0 THEORETICAL DEVELOPMENT

The development presented in this paper uses equations of motion of the two bodies (vehicle and pad) which are uncoupled from one another. The use of such uncoupled equations is more natural conceptually as it allows the two bodies to be treated independently. The free-free vehicle can thus fly off the pad without inducing the compensating forces that are required when a coupled system model is used, and the solution can be obtained in one computer run. However, when the vehicle is on the pad the uncoupled pad and vehicle equations have to be modified to account for the constraints they impose on each other. This necessitates the use of an iterative procedure to converge to a solution, effectively using Lagrange multipliers to apply the required constraints. As the vehicle lifts off the pad the coupling between the vehicle and the pad is eliminated point by point until the vehicle flies free.

### 2.1 EQUATIONS OF MOTION

Write the uncoupled vehicle and stand equations as

$$\begin{bmatrix} M_V & 0 \\ 0 & M_S \end{bmatrix} \begin{pmatrix} \ddot{x}_V \\ \ddot{x}_S \end{pmatrix} + \begin{bmatrix} K_V & 0 \\ 0 & K_S \end{bmatrix} \begin{pmatrix} x_V \\ x_S \end{pmatrix} = \begin{pmatrix} F(t) \\ 0 \end{pmatrix} \quad (1)$$

Assume that the coupling between the vehicle and the main launch pad (MLP) equations is a pure stiffness i.e. the coupling is massless. This coupling stiffness  $K_C$  would overlay the relevant vehicle and stand degrees of freedom when the two are in contact. Equations of motion can now be written as

$$\begin{bmatrix} M_V & 0 \\ 0 & M_S \end{bmatrix} \begin{pmatrix} \ddot{x}_V \\ \ddot{x}_S \end{pmatrix} + \left[ \begin{bmatrix} K_V & 0 \\ 0 & K_S \end{bmatrix} + \begin{bmatrix} K_C \\ \end{bmatrix} \right] \begin{pmatrix} x_V \\ x_S \end{pmatrix} = \begin{pmatrix} F(t) \\ 0 \end{pmatrix} \quad (2)$$

The coupling matrix  $K_C$  can be partitioned out and taken to the right hand side of (2) giving

$$\begin{bmatrix} M_V & 0 \\ 0 & M_S \end{bmatrix} \begin{pmatrix} \ddot{x}_V \\ \ddot{x}_S \end{pmatrix} + \begin{bmatrix} K_V & 0 \\ 0 & K_S \end{bmatrix} \begin{pmatrix} x_V \\ x_S \end{pmatrix} = \begin{pmatrix} F(t) \\ 0 \end{pmatrix} - \begin{bmatrix} K_C \\ \end{bmatrix} \begin{pmatrix} x_V \\ x_S \end{pmatrix} \quad (3)$$

i.e. the coupled system equations have been written in terms of the uncoupled degrees of freedom with a correction term (force) for the effect of interaction between vehicle and stand. This constraint imposed by the interaction of the pad and vehicle now makes the problem suitable for an iterative procedure such as Lagrange multipliers (ref. 2). Application of Lagrange multipliers to the lift-off problem was developed in ref. 3. In the development presented here, because of the very simple assumed nature of  $K_C$  (see section 2.2) Lagrange multipliers do not occur explicitly.

If  $\Phi$  and  $q$  are defined such that

$$x = \Phi q \quad (4)$$

where  $\Phi^T M \Phi = I$

and  $\Phi^T K \Phi = \omega_n^2$

then the modal form of the equations of motion (3) can be written as

$$\begin{bmatrix} 1 & 0 \\ 0 & 1 \end{bmatrix} \begin{pmatrix} \ddot{q}_v \\ \ddot{q}_s \end{pmatrix} + \begin{bmatrix} \omega_{nv}^2 & 0 \\ 0 & \omega_{ns}^2 \end{bmatrix} \begin{pmatrix} q_v \\ q_s \end{pmatrix} = \begin{bmatrix} \Phi_v^T & 0 \\ 0 & \Phi_s^T \end{bmatrix} \begin{pmatrix} F(t) \\ 0 \end{pmatrix} - \begin{bmatrix} \Phi_v^T & 0 \\ 0 & \Phi_s^T \end{bmatrix} \begin{bmatrix} K_C \\ 0 \end{bmatrix} \begin{bmatrix} \Phi_v & 0 \\ 0 & \Phi_s \end{bmatrix} \begin{pmatrix} q_v \\ q_s \end{pmatrix} \quad (5)$$

The second term on the right hand side of the above equation is the contact force term  $F_C$ . Assuming a modal damping ratio of  $\zeta$  the equations can thus be written as

$$\ddot{q} + 2\zeta\omega_n\dot{q} + \omega_n^2q = F_A + F_C \quad (6)$$

If the two bodies are allowed free body motions then the values of  $\omega_n$  corresponding to the rigid body modes are obviously zero. This formulation allows computer core savings because of the diagonalisation of the mass and stiffness matrices. Only small partitions of  $\Phi_v$  and  $\Phi_s$  corresponding to the coupling points are retained in core.

As the vehicle lifts off from the stand and contact is broken point by point, the coupling stiffness  $K_C$  is reduced until, finally, it becomes zero and the vehicle flies free.

## 2.2 COUPLING STIFFNESS MATRIX $K_C$

When the two bodies (vehicle and pad) are in contact they impose constraints on their coupled motion which may be stated as :

- a) Vehicle and pad displacements at the points of contact are equal.
- b) Contact forces have values only at points which are in contact.

These constraints are most easily applied using Lagrange multipliers (refs. 1,3). Their application becomes straightforward if a simple coupling stiffness  $K_C$  is assumed.

Contact points between the vehicle and the pad are shown in figure 1. The function of the coupling stiffness  $K_C$  is merely to constrain the degrees of freedom in contact to move together. A 6 DoF stiffness matrix (3 freedoms each for the SRB and MLP ends of the contact) can serve to provide the required constraints for each contact point. Greater simplification of  $K_C$  is possible if no cross-coupling between the x,y,z freedoms at each end is allowed.

An uncoupled stiffness matrix  $K_C$  automatically satisfies the constraint requirements stated above, and Lagrange multipliers do not occur explicitly in the formulation. Values of  $K_C$  must be chosen to be high relative to the local stiffness values of the two bodies, but yet not so high as to induce spurious responses. The use of an uncoupled stiffness matrix  $K_C$  has an additional advantage in that the reduction of  $K_C$ , as the vehicle lifts off the pad, simply involves zeroing the relevant stiffness terms.

### 2.3 ITERATIVE SOLUTION OF EQUATIONS OF MOTION

Suppose at a given time  $t = t_0$  the solution has been obtained i.e. we know  $q_0, \dot{q}_0$  and the contact force  $F_{C0}$  for a given applied force  $F_{A0}$ .

If  $h$  is the integration interval then at time  $t = t_0 + h$  the new value of applied force  $F_A$  is known. Suppose the stand force needed to satisfy the equations of motion at time  $t = t_0 + h$  is  $F_C$ . Over the interval  $h$  we may approximate the forcing function to  $A + B\tau$ , and the equations of motion become

$$\ddot{q} + 2\zeta\omega_n\dot{q} + \omega_n^2 q = A + B\tau \quad (7)$$

The coefficients  $A$  and  $B$  can be obtained by comparing the above to (6).

At time  $\tau = 0$  the forcing function is  $F_{A0}$  and the contact force is  $F_{C0}$ .

$$\text{Hence } A = F_{A0} + F_{C0} \quad (8a)$$

Similarly at  $\tau = h$ , for the assumed contact force  $F_C$  we can obtain  $B$  as

$$B = \frac{F_A - F_{A0}}{h} + \frac{F_C - F_{C0}}{h} \quad (8b)$$

Closed form solution of equations (7) can be obtained easily in terms of constants  $A$  and  $B$ . For the rigid body modes ( $\omega_n = 0$ ) the equations of motion simply are

$$\ddot{q} = A + B\tau \quad (9)$$

Successive integration gives  $\dot{q}$  and  $q$ .

For the vibration modes of the vehicle the general solution is more complicated; it can be written as

$$q = e^{-\zeta\omega_n\tau} [K_1 \cos \omega_d \tau + K_2 \sin \omega_d \tau] + C + D\tau \quad (10)$$

where

$$\omega_d = \omega_n \sqrt{1 - \zeta^2}$$

$$D = B / \omega_n^2$$

$$C = (A - 2\zeta\omega_n D) / \omega_n^2$$

$$K_1 = q_0 - C$$

$$K_2 = (\dot{q}_0 + \zeta\omega_n K_1 - D) / \omega_d$$

Modal velocity and acceleration can be obtained from (10).

The iterative solution procedure, therefore, is to estimate a value for the contact force at the end of the

integration interval  $\tau = h$ . Coefficients  $A, B$  can then be calculated from (8). These coefficients are used in (9) and (10) to obtain estimated values of  $q$ . Forces and displacements at vehicle-stand interface can then be calculated. Separation of vehicle from the stand is tested for, and a modified coupling stiffness matrix generated. Contact force consistent with the modified coupling stiffness matrix and vehicle displacements is used to obtain new values for constants  $B$  which in turn yield improved estimates for  $q$ ; the process is repeated until the stand force obtained between successive iterations is within a specified tolerance, indicating that the solution has converged to the required accuracy.

## 2.4 TEST FOR CONVERGENCE

If the solution has converged, the right hand side of equation (6) has to be equal to its left side. If the two are not equal then the error is

$$\eta = F_A + F_C - \ddot{q} - 2\zeta\omega_n\dot{q} - \omega_n^2q$$

If  $F_{Ci}$  denotes the stand force estimate from the previous iteration, and  $F_{Cj}$  the stand force from the current iteration then, substituting for  $\ddot{q}, \dot{q},$  and  $q$  in terms of  $A$  and  $B$  gives the error between successive iterations as

$$\eta = F_{Cj} - F_{Ci} \tag{11}$$

i.e the error in successive iterations is simply the difference in the contact force. The solution may be said to be converged if the value of the error becomes sufficiently small; for our purposes a satisfactory error criterion was a difference of less than 1 lbf. between successive iterations.

## 2.5 DETERMINATION OF INTEGRATION STEP SIZE

Because the error between successive iterations is in the stand force the integration step size need only be small enough to track the highest frequency in the contact force. An estimate of the oscillatory behaviour of the vehicle on the pad is obtained by reducing the mass and stiffness properties of the two bodies to the stand interface points and coupling the two appropriately. The highest frequency from the resulting eigensolution governs the integration step size :

$$h \leq 0.25 / f_h \tag{12}$$

where  $f_h$  is the highest frequency so obtained.

## 2.6 INITIAL CONDITIONS

Initial conditions are most easily obtained by solving the static problem of the vehicle resting on the pad. They can be compared to the response obtained from the method itself by allowing the vehicle to settle under the action of applied static loads; mean values of the resulting oscillations should be the same as obtained statically, providing a good check on the computer code and the models.

## 2.7 SEPARATION AND RECONTACT CRITERIA

Conditions governing the behaviour of the contact points between the pad and the vehicle are easily established when using the uncoupled stiffness matrix  $K_C$ .

When the vehicle is bolted to the pad the contact point can sustain both tensile and compressive loads. Once the SRB bolts have been fired, the contact point becomes non-linear in that no tensile loads can be sustained. Contact between the vehicle and the pad is thus assumed broken as soon as the bolt goes into tension.

The condition for reattachment is similarly simple. Because of the assumed nature of  $K_C$  (no cross coupling) a check of relative displacements between the two bodies shows when recontact takes place. However on recontact, to simulate the sliding joint between the vehicle and the pad, only axial (normal) loads were permitted because otherwise any lateral drift would induce spurious forces.

## 3.0 GENERATION OF LAUNCH ANALYSIS MODELS

Each component of the launch vehicle was modeled mass coupled in mixed modal and discrete coordinates using the Craig-Bampton method (ref. 4). Using this method a set of freedoms, called the boundary freedoms, are grounded and an eigensolution obtained of the remaining DoFs. From this eigen a number of significant modes are retained. A dynamics model is then constructed using the retained modes and the boundary set of retained freedoms. The resulting mass and stiffness matrices are of the form

$$M = \begin{bmatrix} I & C_M \\ C_M^T & M_B \end{bmatrix} \quad K = \begin{bmatrix} \omega_n^2 & 0 \\ 0 & K_B \end{bmatrix} \quad (13)$$

Some very important points need to be noted in the generation of such models. Any freedoms which have large concentrated loads (e.g. SSV major interfaces) must be retained as discrete. Contact points, which require high fidelity results to properly simulate separation and recontact, must also be kept explicitly. A reduction of the remaining degrees of freedom is permissible as indicated above using the Craig-Bampton method, with an eigensolution and the retention of only the important modes. This mode selection is often by simple frequency bandpass, but other criteria can be employed. Finally, since the launch vehicle will have large rigid body motions, the stiffness of each component must be truly free-free to inhibit the build-up of spurious forces.

Component models are assembled into a launch vehicle model by overlaying the common boundary freedoms. The launch vehicle model is then eigensolved with properties as in equation (4) to diagonalise the mass and stiffness matrices. All modes from this final eigensolution are retained for further analysis.



#### 4.0 EXTERNAL FORCING FUNCTIONS

Any dynamic system is subject to forcing functions which can be constant or time varying. The determination of these forcing functions is usually the most difficult part of any dynamics problem. The launch vehicle is subject to a number of external influences most of which have been refined over the years and are well known. How these various forces are dealt with is described in this section.

#### 4.1 DATABASE FORCING FUNCTIONS

A computer tape containing the NASA launch analysis forcing functions was obtained from MSFC. There was data for 11 lift-off cases, comprising engine forcing functions, winds and gusts.

This forcing function data, which is standard for SSV launch analysis, was converted to generalised forcing functions using the final free-free vehicle modal matrix. The data was read as required during the execution of the computer program.

#### 4.2 GRAVITY LOADS

Gravity loads can be obtained easily for the mass coupled models as generated using the Craig-Bampton method. A geometric rigid body modeshape of the model can be constructed, bearing in mind that, since the modes are obtained for zero boundary motion, the geometric modeshape corresponding to the modal freedoms is zero. The gravity loads are then obtained from the mass matrix as

$$FG = \begin{bmatrix} I & C_M \\ C_M^T & M_B \end{bmatrix} \begin{bmatrix} 0 \\ RB \end{bmatrix} \{g\} = \begin{bmatrix} C_M \\ M_B \end{bmatrix} [RB] \{g\} \quad (14)$$

Thus the discrete mass of the vehicle, which causes gravity loads, is inherent in the column partition of the mass matrix corresponding to the boundary freedoms. This method allows very easy calculation of vehicle gravity loads.

#### 4.3 CRYOGENIC LOADS

Cryo loads are generated at the SRB to MLP boundary because of the restraints imposed on shrinkage of the ET as the cold propellents are loaded. As the vehicle lifts off these restraints are removed and the SRBs twang inwards. Any technique for cryo load application should properly simulate this behaviour. This was achieved simply by applying the cryo loads to the ET itself such as to shrink the tank. Structural flexibility allows the loads to be distributed properly through the vehicle, and produces the required cryo reaction loads at the SRB base.

Since the cryo loads are a function of the structural stiffness, and are not related to the mass matrix, they must be applied only at the discrete freedoms of the mass-coupled component modal model. Otherwise, spurious modal distortions are obtained.

Cryo loads were assumed to be steady state and were added to the gravity force vector to give the total constant force on the vehicle.

#### 4.4 CONTROL SYSTEM

The vehicle control system directs SRB gimbaling to zero out any net moments about the vehicle centre of gravity. The formulation given in this section was developed to simulate the effect of the control system in maintaining a vertical attitude of the launch vehicle during the first few seconds of flight.

Using the geometric rigid body modeshape  $RB$  the resultant force vector  $P_R$  at the c.g. of the vehicle is obtained from the physical applied forces  $P_A$  as

$$P_R = RB^T P_A \quad (15)$$

This vector may be written in terms of its three force and three moment components as

$$P_R = \begin{pmatrix} F_R \\ M_R \end{pmatrix} \quad (16)$$

The control system action is such that the resultant moments  $M_R$  vanish subject to the constraint that the corrective forces are applied only at the lateral (y,z) freedoms at the SRB gimbals. Forces required to produce a moment of  $-M_R$  are obtained by relating  $x_{sl}$ , the SRB lateral gibal freedoms, to the freedoms at the c.g. of the vehicle with the geometric rigid body modeshape as

$$x_{sl} = RBL x_g$$

where  $RBL$  is the appropriate partition of  $RB$ . Hence we can write

$$\begin{aligned} x_g &= (RBL^T RBL)^{-1} RBL^T x_{sl} \\ &= T1 x_{sl} \end{aligned} \quad (17)$$

As only the partition of  $T1$  corresponding to the rotational degrees of freedom ( $T1R$ ) is needed to zero out the net moments about vehicle c.g. the above can be written as

$$x_{gr} = T1R x_{sl} \quad (18)$$

Using the corrective moment required we can obtain  $FSL$ , the SRB lateral forces, as

$$\begin{aligned} FSL &= -T1R^T M_R \\ &= -T1R^T RBL^T P_A \end{aligned} \quad (19)$$

However, during computation, the forcing functions are known as generalised quantities. Using the final free-free modes discrete forces can be obtained from generalised as

$$P_A = \Phi^{-1T} F_A \quad (20)$$

The inverse of the modal matrix  $\Phi$  can be obtained easily from its properties. For mass normalised modes

we have

$$\Phi^T M \Phi = I$$

Hence  $\Phi^{-1} = \Phi^T M$

thus reducing the process of inversion to that of multiplication. Now we can write the discrete SRB corrective forces as

$$FSL = -T1R^T RBL^T \Phi^{-1T} F_A \quad (21)$$

The corrective forces FSL in equation (21) are converted to generalised forces for use in the lift-off program.

#### 4.5 GRAVITY SOFTENING

Because of the offset c.g. of the vehicle, deflection of the c.g. from its null position will induce a further bending moment in the structure, which in turn will lead to extra deflection. This effect may be viewed as a softening of the structure under gravity loading and could be important as the vehicle rocks on the pad when the Space Shuttle main engines (SSMEs) are lit.

Implementation of the gravity softening effect was as for the control system. As before we can relate the motion of the vehicle c.g. to the motion of the boundary freedoms  $x_b$  using the rigid body mode shape

$$x_b = RB x_g$$

Hence  $x_g = (RB^T RB)^{-1} RB^T x_b$

$$= T2 x_b \quad (22)$$

This relationship is assumed to hold even for the deformed vehicle i.e. for small deflections.

Using the final free-free modes of the vehicle the boundary freedoms are related to the modes as

$$x_b = \Phi_b q$$

where  $\Phi_b$  is the partition of the modal matrix corresponding to the boundary freedoms. Hence the motion of the c.g. is obtained in terms of modal freedoms as

$$x_g = T2 \Phi_b q$$

$$= ERV q \quad (23)$$

The translational and rotational components of c.g. motion can be written as

$$\begin{pmatrix} x_{gt} \\ x_{gr} \end{pmatrix} = \begin{bmatrix} ERVt \\ ERVr \end{bmatrix} \{q\} \quad (24)$$

The translational deflection  $x_{gt}$  obtained from the above equation causes an additional moment because of the motion of the centre of gravity (gravity force application point). This moment may be written in matrix form as

$$\begin{aligned} M_G &= \begin{bmatrix} 0 & -FGZ & FGY \\ FGZ & 0 & -FGX \\ -FGY & FGX & 0 \end{bmatrix} \{x_{gt}\} \\ &= FGM \ x_{gt} \end{aligned} \quad (25)$$

Using the relationships developed in (24) and (25) the generalised moment due to deflection of the c.g. is given by

$$\begin{aligned} FSOF &= ERVr^T M_G \\ &= ERVr^T FGM ERVt \ q \end{aligned} \quad (26)$$

The "softening stiffness" is thus obtained as

$$KSOF = ERVr^T FGM ERVt \quad (27)$$

For static calculation of initial conditions  $KSOF$  is used in conjunction with the linear elastic stiffness of the vehicle to obtain extra deflection because of its off-set centre of gravity. The effect of gravity softening on the deflection of the vehicle c.g. is shown in table 1.

In the response calculations the softening effect is considered to be an extra applied force and is carried on the right hand side of the equations of motion. This force is obtained from equation (26) above; if the matrix multiplications are carried out from the right the process is very quick and requires just the small amount of core needed by  $ERV$  and  $FGM$ . To avoid numerical stability problems  $FSOF$  was considered to be constant over an integration interval (typically 0.0001 sec.).

The gravity softening effect was turned off at SRB ignition.

## 5.0 APPLICATIONS AND RESULTS

The computer code generated with this methodology has been used in a number of diverse applications. The main effort was in obtaining launch loads for a SSV with an Aft Cargo Carrier attached to the aft frame of the ET; the payload in the ACC was an Orbital Transfer Vehicle (OTV). Figure 2 is an illustration of the ACC-OTV concept. Figure 3 shows one of the loads responses between the ET and the aft SRB attachment. Loads generated on an OTV propellant tank are shown in figure 4. The hydroelastic volume change in the ullage space of the liquid oxygen tank of the ET due to the lift-off transient is shown in figure 5; the oscillation in the tank bottom pressure is shown in figure 6. The primary mode in both these phenomenon is the 4Hz first bulge mode of the tank. Figures 3-6 illustrate the severity of response when

the SRBs are lit ( 6.6 sec in the plots). These responses correlate well with the results obtained by other independent analyses.

The program was used to calculate barge impact loads and ET response during docking procedures in the harbour at VAFB. A sketch of the barge and the dock is shown in figures 7 and 8. It was assumed that the barge had an initial velocity imparted by a wave. The barge was then allowed to impact a dock of various stiffness values. It was found that the loads generated at the ET transporter interfaces were acceptable even for severe impact cases. The dock impact loads were governed by the barge stiffness for a stiff dock, and by the dock stiffness for a soft dock. The impact wave as it travels through the deck of the barge is shown in figure 9.

## 6.0 CONCLUDING REMARKS

Results obtained by the method developed in this paper have been shown to be in good agreement with observed loads and other analysis methods.

The resulting computer program has general applicability, and has been used without modification to solve a variety of contact problems. The contact point description could be made more elaborate to include effects of friction, geometry, etc. By allowing the second body (it need not be a pad) to have rigid body free-free modes other problems, such as berthing/docking dynamics, could be tackled.

## 7.0 REFERENCES

- 1) Prabhakar, A " Development of a lift-off response program to obtain launch loads for ACC-OTV ", MMC Michoud IOM 3524-85-260
- 2) Halfman, R L "DYNAMICS VOL II", Addison-Wesley 1962
- 3) White, C W and Bodley, C " Boundary interchanges between redundantly connected complex structures ", MMC Denver R78-48628
- 4) Craig, R R and Bampton, M C C "Coupling of substructures for dynamic analyses", AIAA Journal Vol. 6 No. 7 July 1968

VEHICLE C.G. MOTIONS UNDER STATIC LOADS

	X (in)	Y (in)	Z (in)
1) GRAVITY ONLY ①	-1.174	-0.053	-1.531
2) ① + G-SOFTENING	-1.179	-0.058	-1.726
3) ① + CRYO	0.184	-0.050	-0.923
4) ① + G-SOFTENING + CRYO	0.181	-0.057	-1.060

C-3

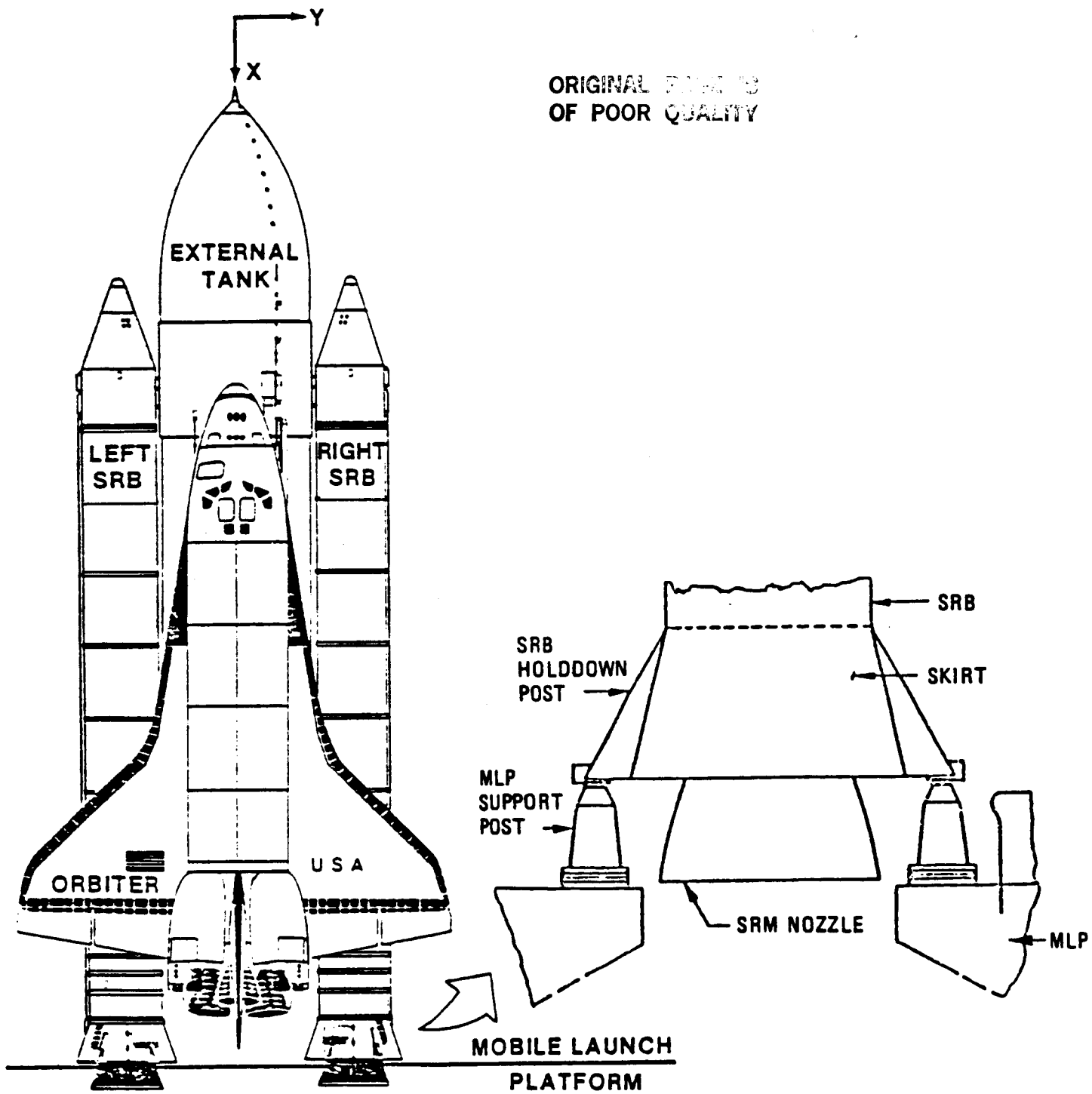


FIGURE 1 TOP SIDE VIEW OF THE SPACE SHUTTLE VEHICLE

AFT CARGO CARRIER CONCEPT

ORIGINAL PAGE IS  
OF POOR QUALITY

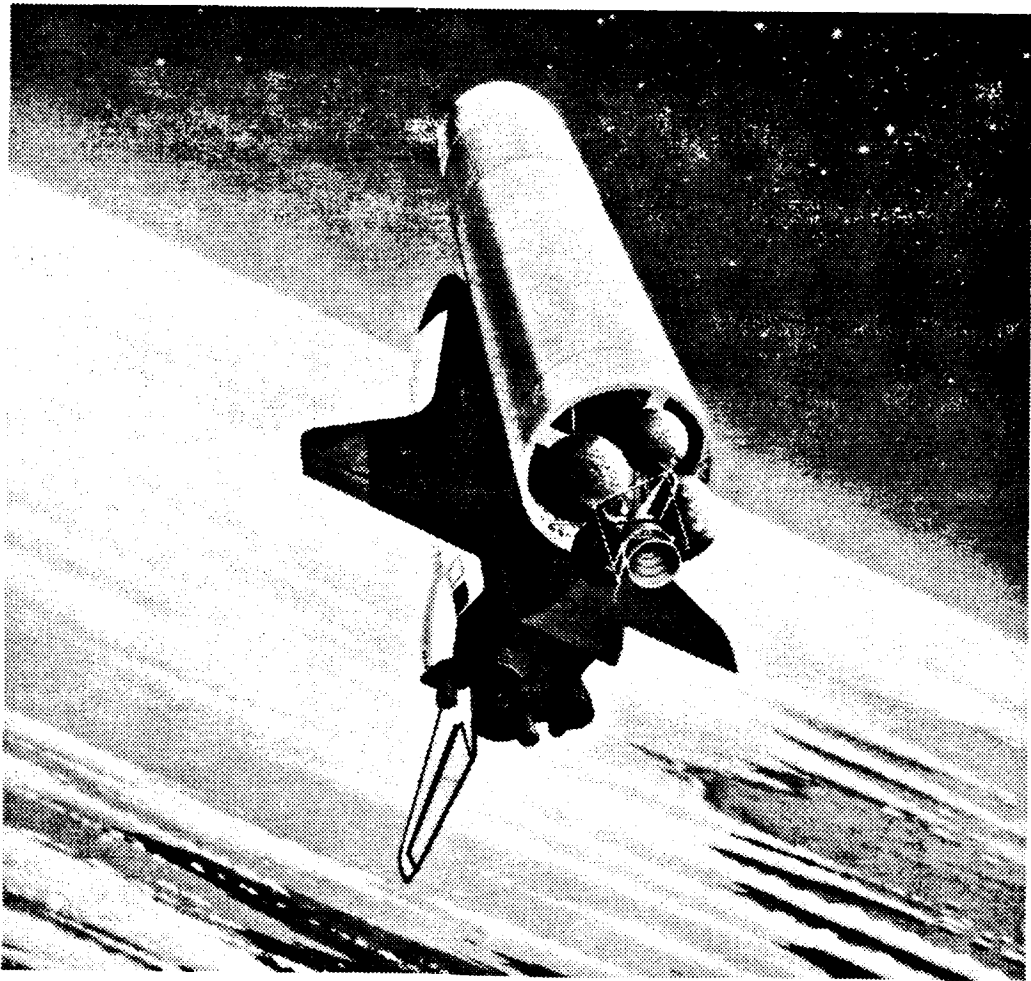
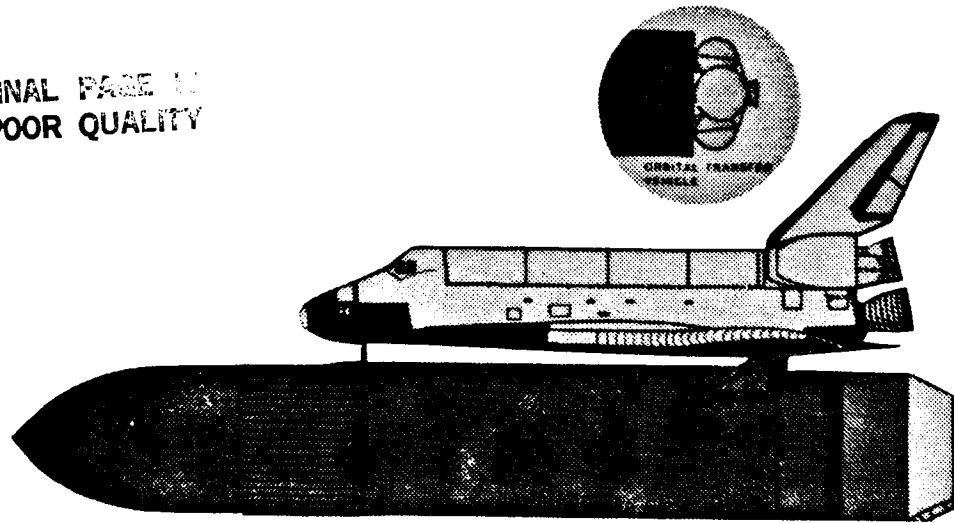


FIGURE 2



ACC-OTV LAUNCH TRANSIENT ANALYSIS  
ET/SRB UPPER Y FORCE

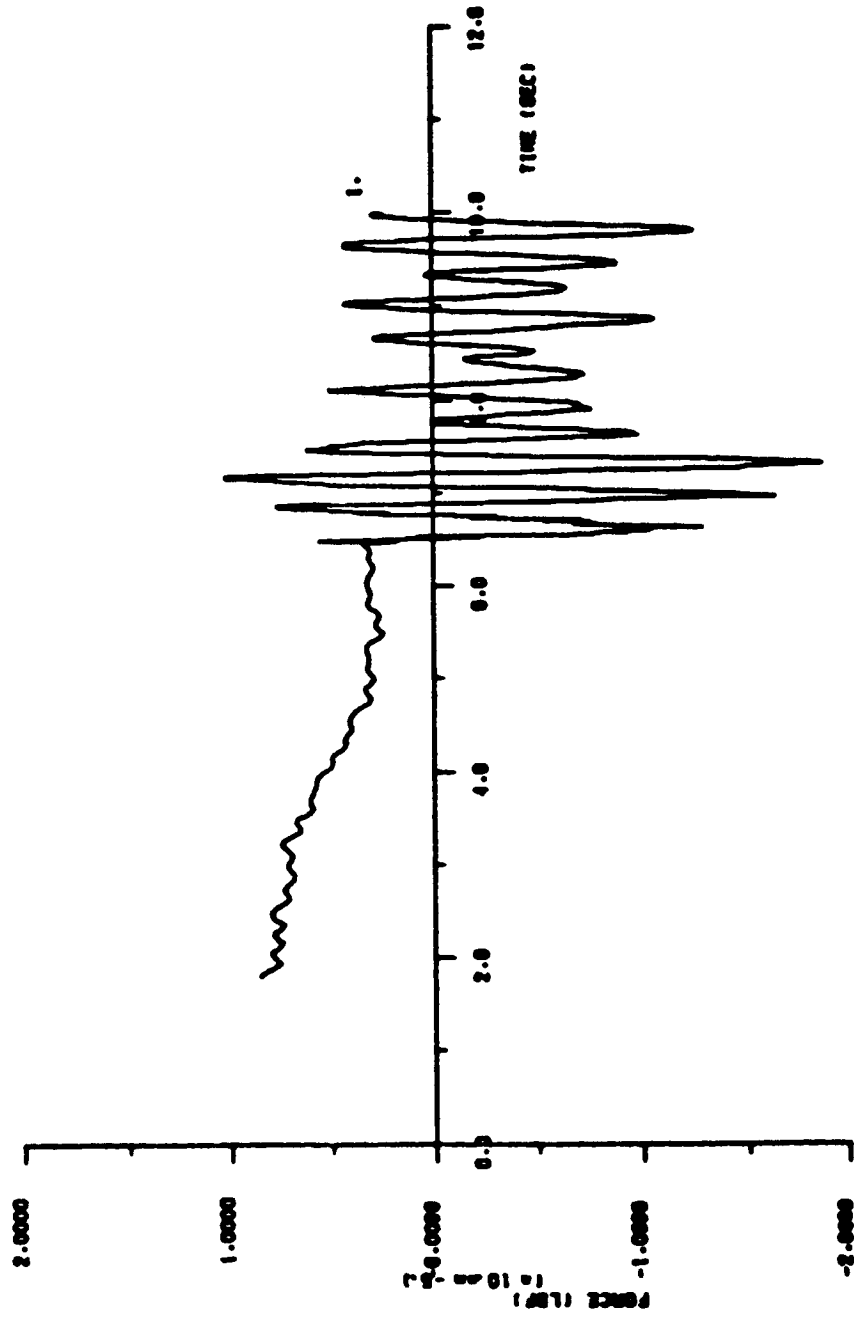


FIGURE 3

ACC-OTV LAUNCH TRANSIENT RESPONSE ANALYSIS  
OTV UPPER LOX TANK X FORCE

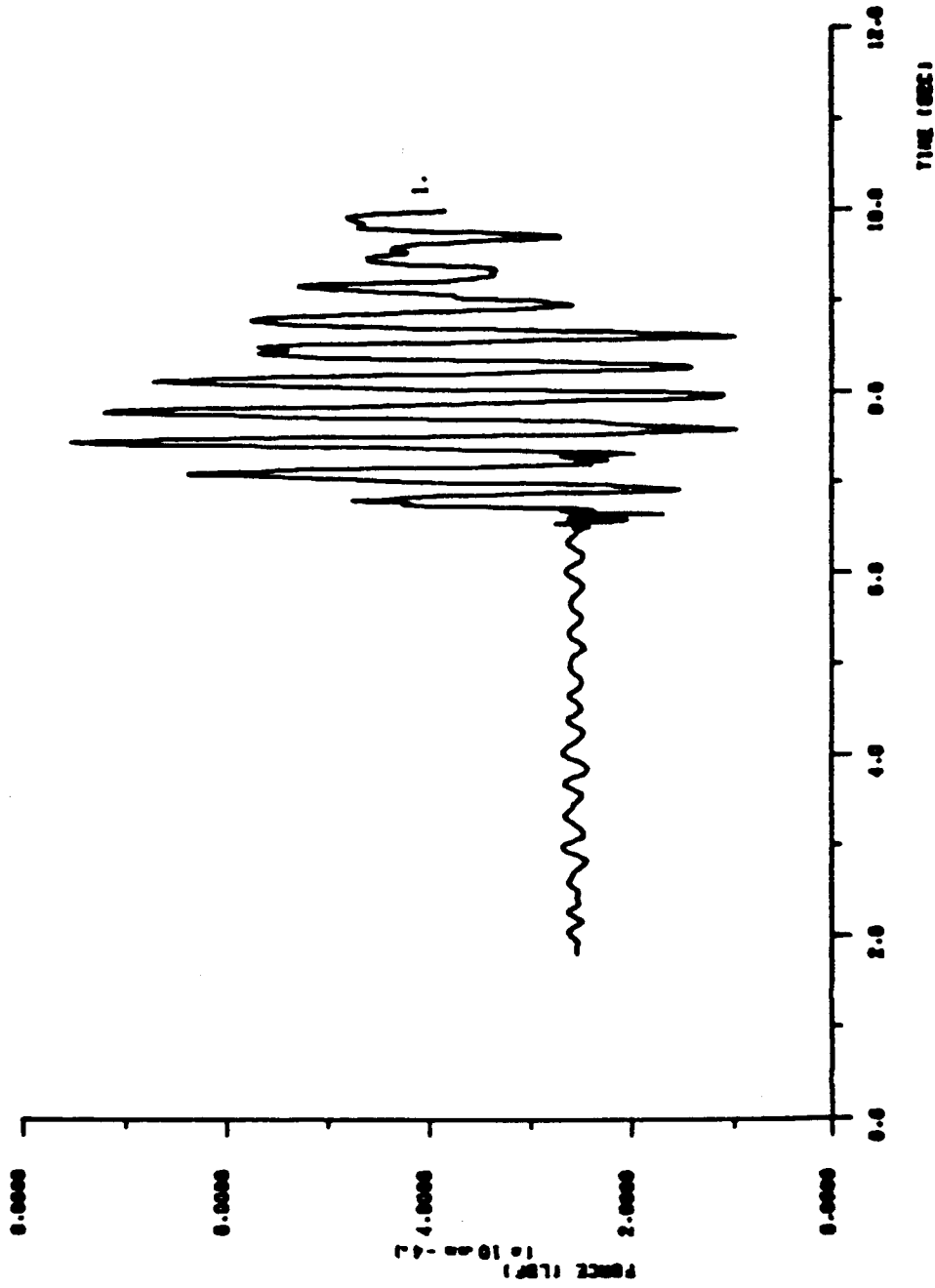


FIGURE 4

LOX TANK PRESSURE SLUMP ANALYSIS - LIFT-OFF TRANSIENT  
ULLAGE SPACE VOLUME OSCILLATION

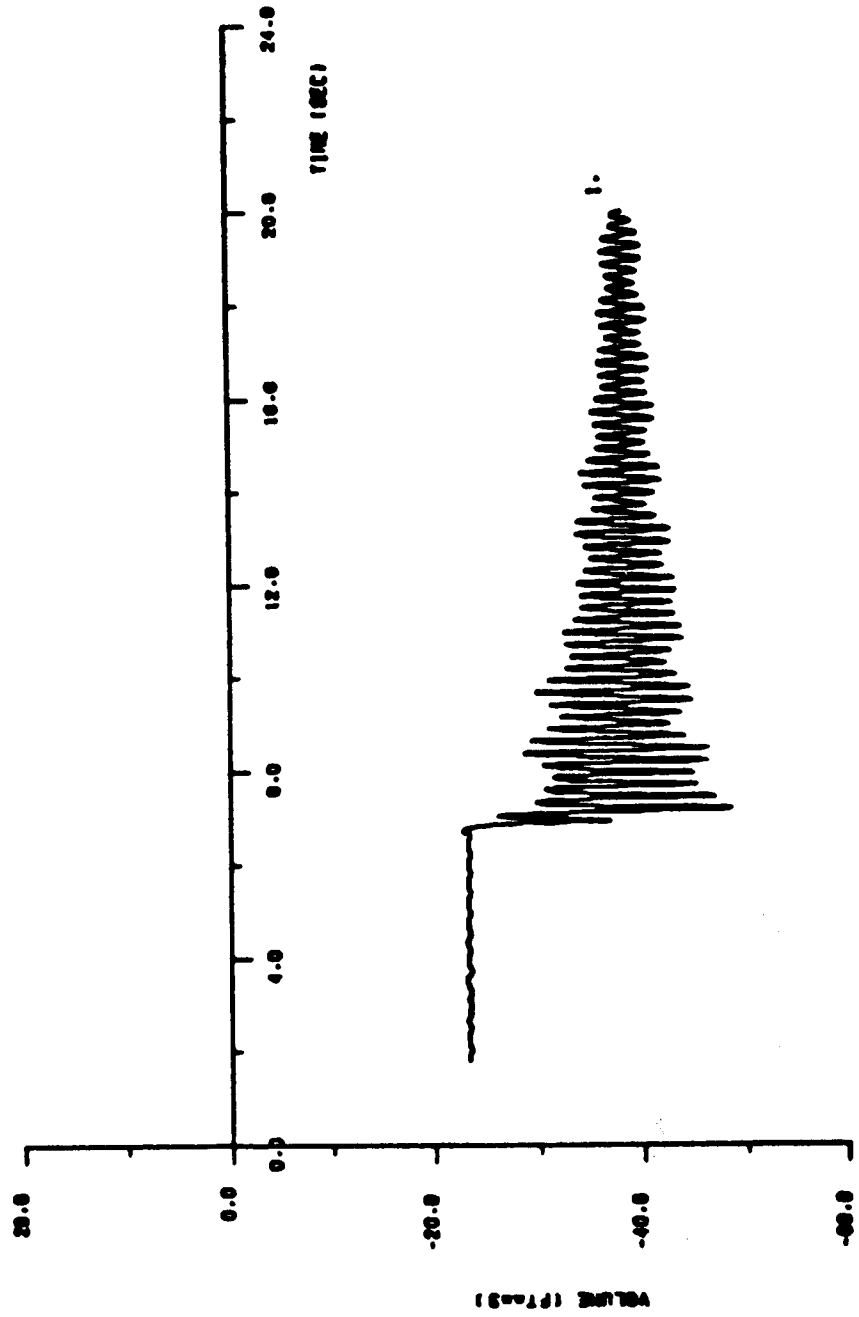


FIGURE 5

LOX TANK PRESSURE SLUMP ANALYSIS - LIFT-OFF TRANSIENT  
TANK BOTTOM PRESSURE

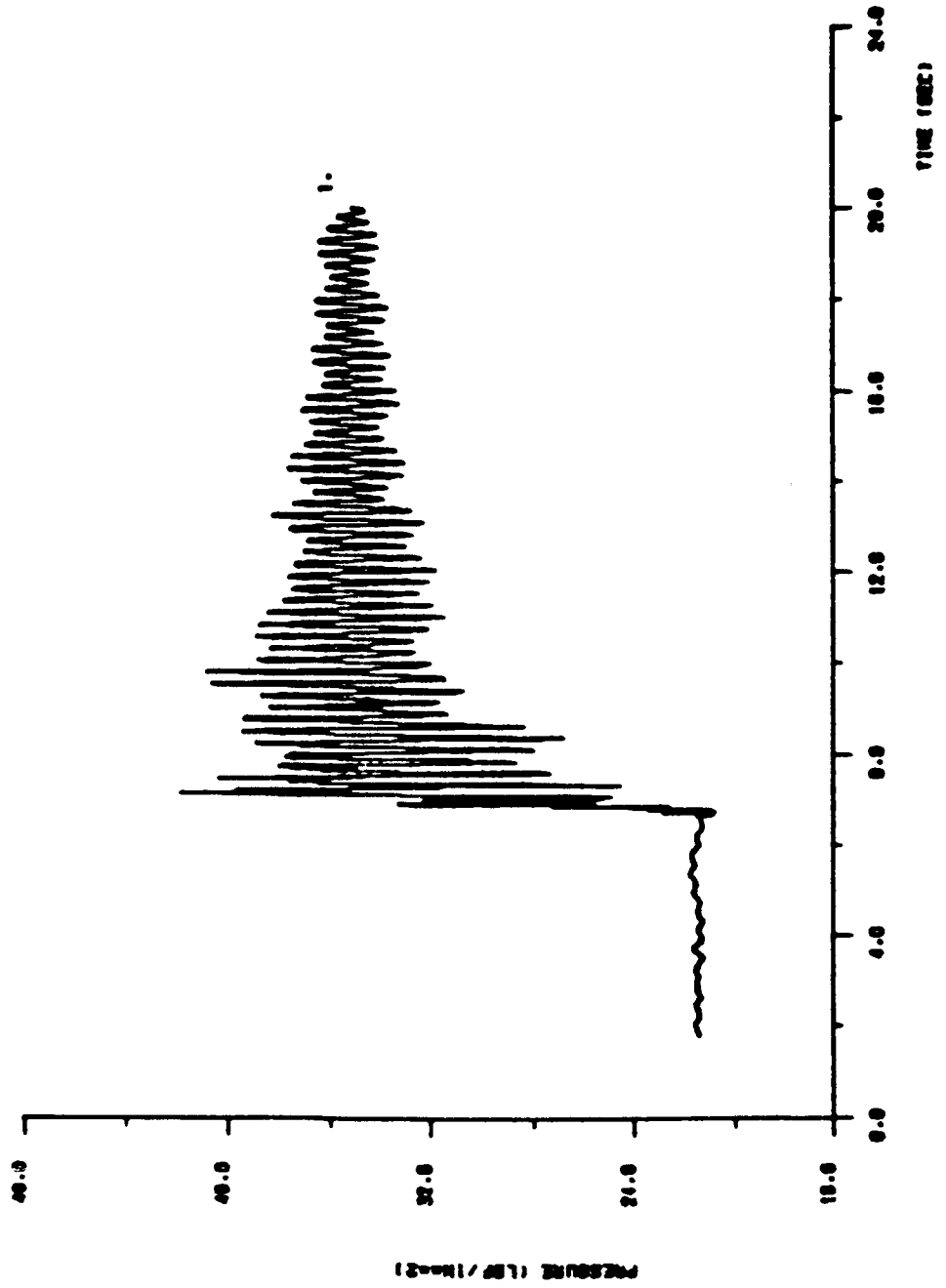
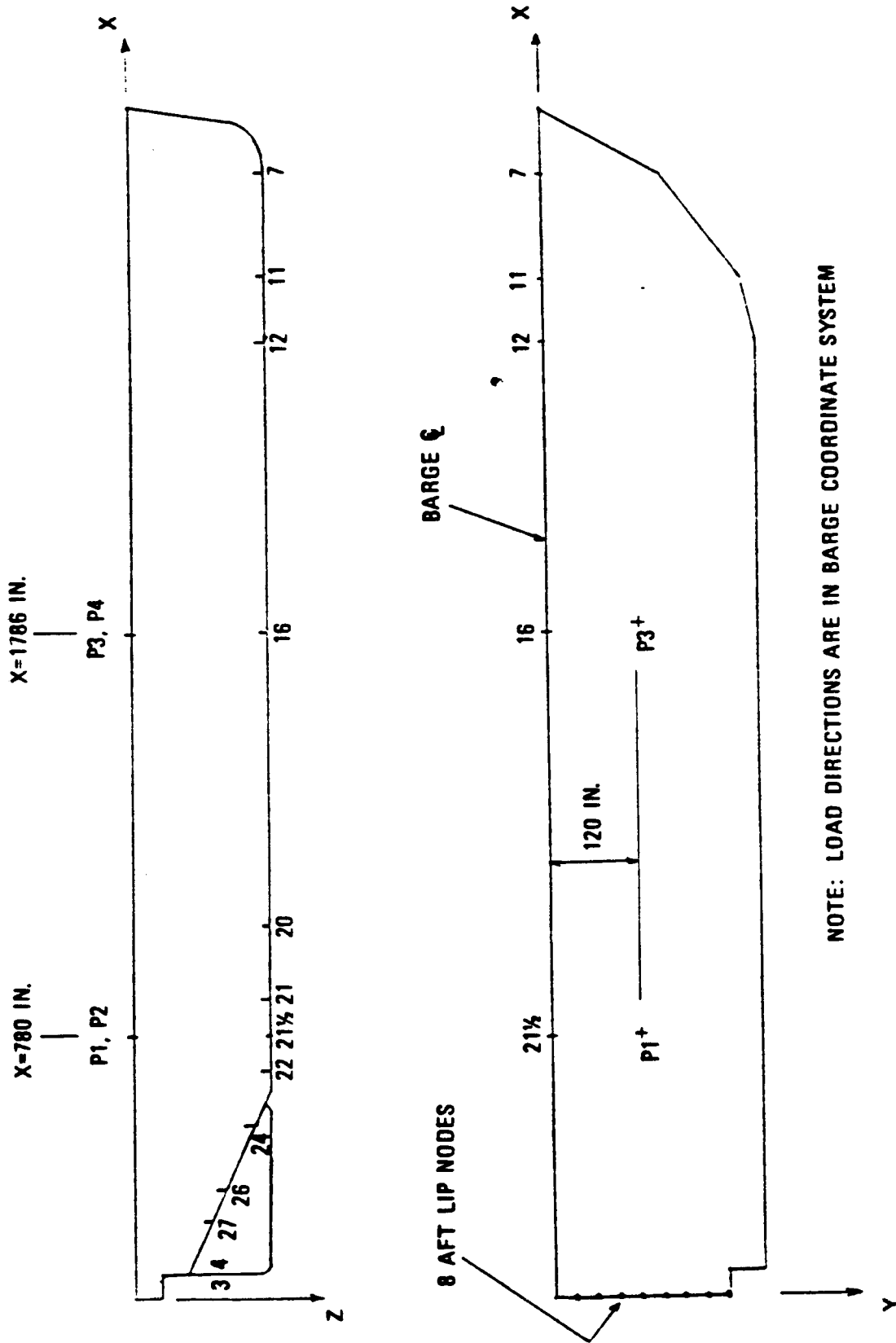
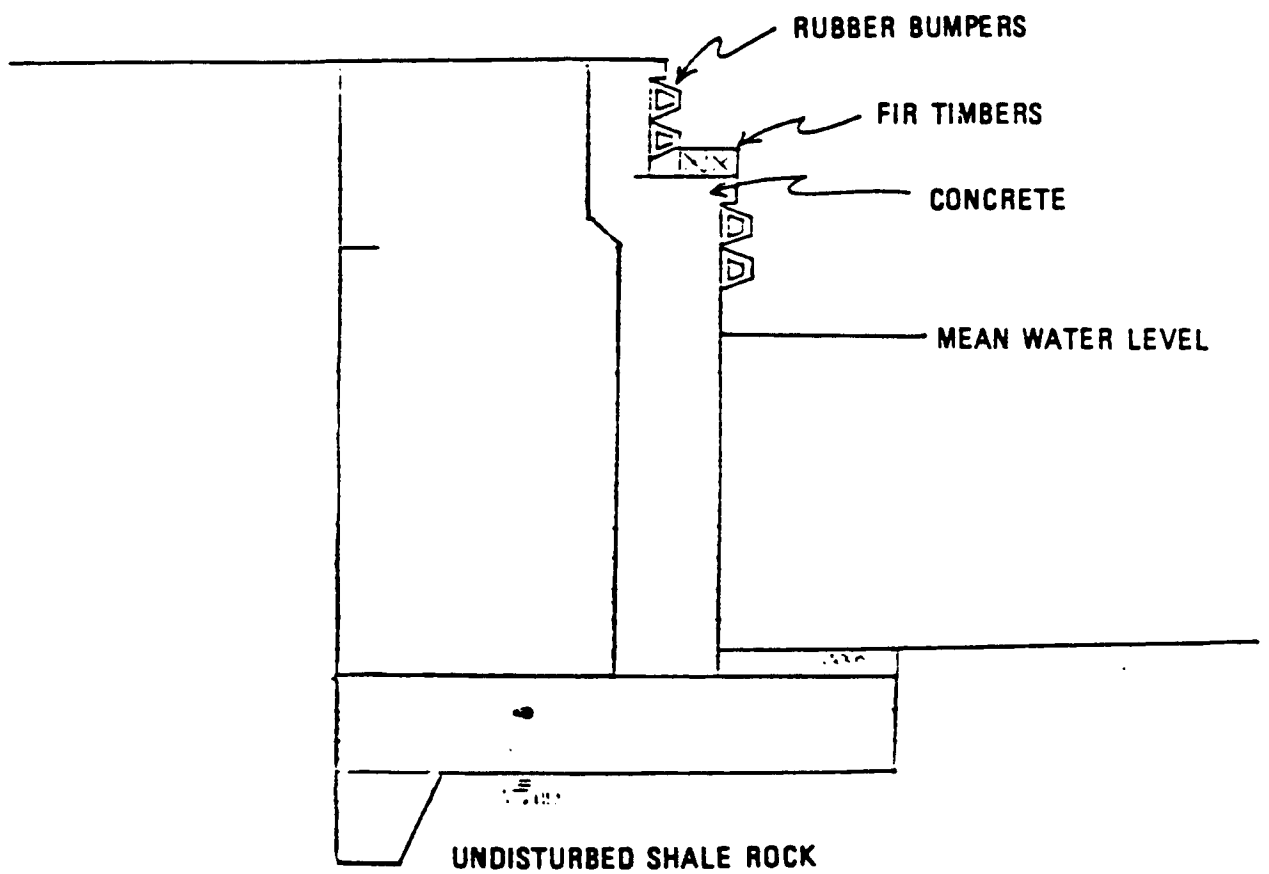


FIGURE 6

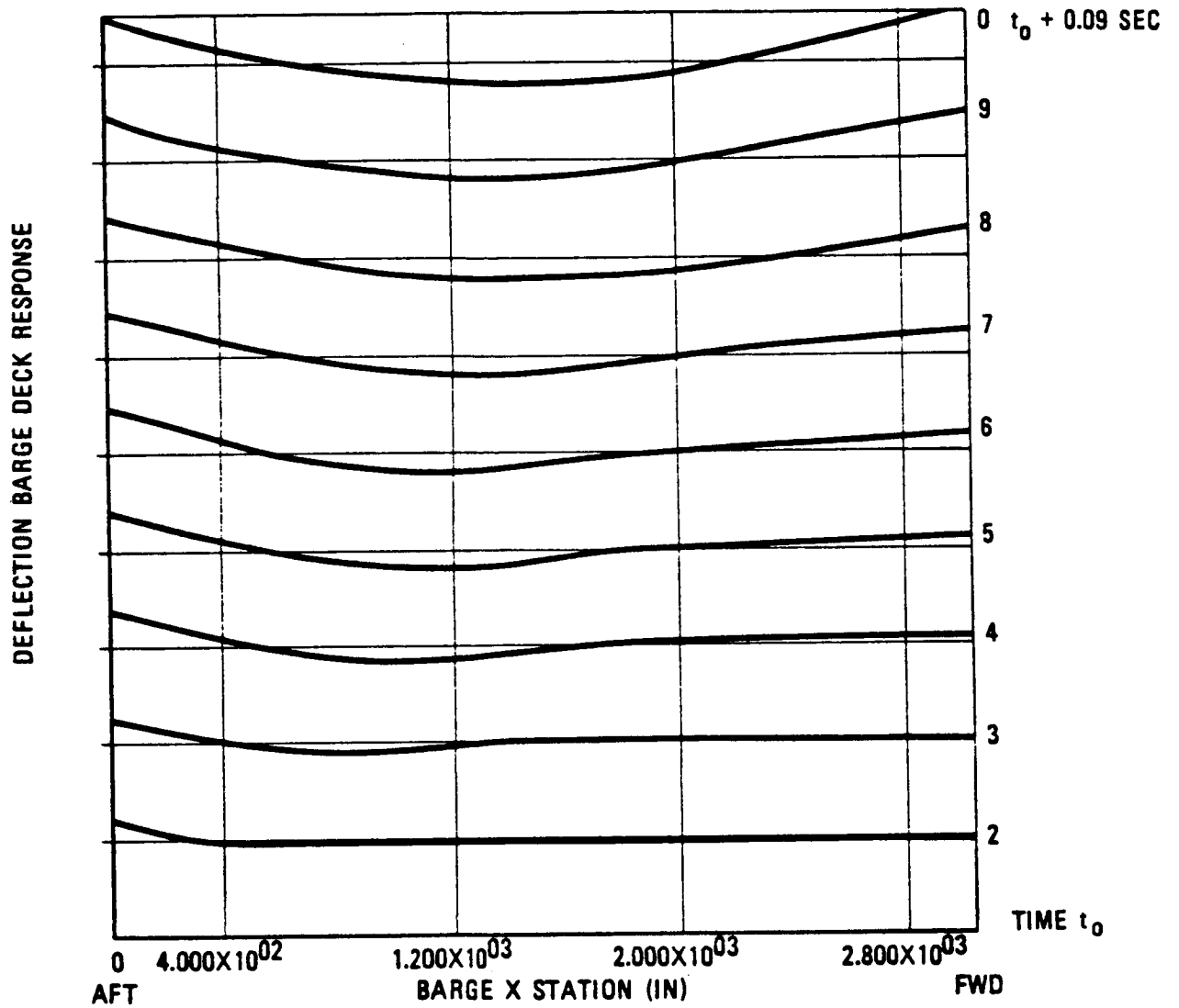


NOTE: LOAD DIRECTIONS ARE IN BARGE COORDINATE SYSTEM

FIGURE 7: BARGE RESPONSE LOCATIONS



**FIGURE 8: VAFB DOCK CROSS SECTION**



BARGE DECK RESPONSE FOR A 12 IN./SEC Z IMPACT

FIGURE 9